Bounds on the Delay-Constrained Capacity of UWB Communication with a Relay Node

Zolfa Zeinalpour-Yazdi, *Student Member, IEEE*, Masoumeh Nasiri-Kenari, *Member, IEEE*, Behnaam Aazhang, *Fellow, IEEE*, Joachim Wehinger, *Member, IEEE*, and Christoph F. Mecklenbräuker, *Senior Member, IEEE*

***Abstract*—We derive bounds on the expected capacity and outage capacity of a three-node relay network for UWB communications. We also provide a simple tight approximation for the derived upper bound on the capacity and then using this bound we obtain the outage probability of the network. Numerical results show that a significant improvement in the system capacity and outage probability is obtained by adding a relay node. Moreover, our theoretical results reveal that the diversity gain of a relay channel substantially increases by using UWB links instead of NB links. We also derive these bounds when we have a constraint on the total transmitted power of the source and the relay nodes.**

***Index Terms*—UWB channel, relay channel, expected capacity, outage capacity, outage probability, power constraint.**

I. Introduction

ULTRA-WIDEBAND (UWB) radio is a promising technology to meet the recent interest in low-cost, low-power, and low-latency wireless links for short range communications. However, such systems face major challenges to achieve a desired level of reliability and throughput. In wireless networks, diversity techniques are used to improve link reliability. In meshed communication networks, diversity can be achieved by *cooperative* transmission [1], [2].

The simplest cooperative network is the three terminal relay network. Many capacity bounds for the relay channel have been derived for a flat fading channel [3], [4], [5]. Motivated by [5], we study bounds for a frequency-selective block-fading UWB channel [6]. Note that for our model (bounded codeword lengths) Shannon capacity can be used in the framework of outage and expected capacities (the expectation is carried out with respect to the random channel state) [7].

Cooperative diversity was studied in [8] for relaying over slow Rayleigh fading channels focusing on outage performance at low SNR. The term *outage* refers to the event that the channel state cannot support a required data rate. Outage capacity was shown to be achievable by a modified "bursty" amplify–forward protocol without prior channel knowledge at the receivers. Following [8], we consider outage probability as a suitable performance limit indicator, especially in slow fading channel and short codeword length. Achievable rates using amplify-and-forward (AF) with network training are analyzed in [9] for narrow– and wideband relaying over frequency-selective fading channels. Large scale wireless sensor networks using efficient flooding are investigated in [10]. Therein, it is shown that the upper bound on the probability of decision error at the fusion center can decrease exponentially with increasing the number of nodes.

Here, we compute upper and lower bounds on the expected and outage capacities[1] of a simple relay network with realistic UWB links. Using these results we subsequently obtain a closed form lower bound on the outage probability. Further, we allow the total available transmit power of the source and relay to be optimally split between the nodes and study the resulting capacity bounds. The paper is organized as follows: Sec. II defines the relay network and UWB channel model. Upper and lower bounds on the capacity are derived in Sec. III. In Sec. IV, we present a lower bound on the outage probability of the system. We derive upper and lower bounds on the above capacities while we have a constraint on the transmitted power in Sec. V. Finally, we evaluate these bounds numerically in Sec. VI and provide the conclusion in Sec. VII.

Notation: The mutual information rate is denoted by $I(\cdot)$ and the differential entropy by $h(\cdot)$. We use *bit* as the unit of information and all logarithms are defined with base 2. The superscripts $(\cdot)^*$ and $(\cdot)^T$ are used to denote complex conjugate and transpose, respectively. The operators $\mathbb{E}\{\cdot\}$, $\Re\{\cdot\}$, and $\mathrm{var}(\cdot)$ are expectation, real part, and variance, respectively. We use $\lfloor x \rfloor$ to denote the largest integer value $\leq x$.

II. System Model

Consider the UWB-linked relay network, in which the source S wants to transmit a UWB signal to the destination D (via link1) with the assistance of a relay R. Imposing a K-block delay-constraint on the system requires that the data transmission occurs in frames of K-blocks. Data is encoded (by a codebook of size K) and transmitted as an impulse-based UWB signal by the source. The relay node receives the UWB signal from the source perturbed by multipath fading

Manuscript received May 21, 2008; revised September 21, 2008; accepted October 30, 2008. The associate editor coordinating the review of this letter and approving it for publication was A. Nallanathan.

Z. Zeinalpour-Yazdi and M. Nasiri-Kenari are with the Department of Electrical Engineering, Sharif University of Technology, Tehran, Iran (e-mail: zeinalpour@ee.sharif.edu).

B. Aazhang is with the Department of Electrical and Computer Engineering, Rice University, Houston, TX 77251 USA.

J. Wehinger is with Infineon Technologies, Munich, Germany.

C. F. Mecklenbräuker is with the Vienna University of Technology and the ftw. Telecommunication Research Center, both in Vienna, Austria.

This paper was presented in part at the Asilomar Conference on Signals, Systems, and Computers, October 29-November 1, 2006.

Digital Object Identifier 10.1109/TWC.2009.080682

[1]We actually obtain bounds on the achievable rates. For simplicity we will refer to these as bounds on the capacity.

and additive white Gaussian noise (link2). Then, it decodes the received signal and transmits an auxiliary UWB signal (via link3) for aiding the data transmission from the source to the destination, using a set of relay functions which depend only on the past received signals at the relay [3]. Finally, the destination observes a superposition of the UWB signals from the source and the relay, and jointly processes all its observations to infer the data which was initially encoded by the source. Throughout the paper, we assume that all nodes are perfectly synchronized and also CSI is available at receiving terminals only.

We adopt the multipath channel model specified by the IEEE 802.15.4a group for the evaluation of the physical layer of UWB [6]. The impulse response of this model is [6]

$$h(t) = \widetilde{\beta} \sum_{\ell=0}^{L-1} \sum_{m=0}^{M-1} a_{m,\ell} e^{j\phi_{m,\ell}} \delta(t - T_\ell - \tau_{m,\ell}), \qquad (1)$$

where T_ℓ and $\tau_{m,\ell}$ represents the cluster and ray arrival times, and they follow Poisson distribution and mixtures of two Poisson distributions (with mixing factor β), respectively. The factor $\widetilde{\beta}$ jointly models the pathloss, shadowing, and antenna insertion loss. The distribution of the gain of the mth path in the ℓth cluster, *i.e.*, $a_{m,\ell}$, is Nakagami with parameter m [11], which is modeled as a lognormally distributed random variable and finally the phase $\phi_{m,\ell}$ is taken as a uniformly distributed random variable from the range $[0, 2\pi]$. The detail of joint probabilistic model of these parameters is tabularized in [6]. In our analysis, we assume that the receiver is capable of capturing all multipath components. We know that if the transmitter sends a block of K symbols $(x_0, \ldots, x_{K-1})^T$ through the above UWB channel, the receiver will observe $(y_0, \ldots, y_{K-1})^T$ [12]

$$y_i = \sum_{k=0}^{K'-1} g_k x_{i-k} + z_i \quad (i = 0, \ldots, K-1) \qquad (2)$$

where z_is are zero mean complex additive white Gaussian noises, K' is the ISI length due to the multipath fading, and g_ks are related to the channel impulse response as

$$g_k = \sum_{i,\ell:\lfloor d_{i,\ell}/T_s \rfloor = k} \widetilde{\beta} a_{i,\ell} e^{j(\phi_{i,\ell} - 2\pi f_c d_{i,\ell})}. \qquad (3)$$

In this equation, $d_{i,l} = T_l + \tau_{i,l}$, and $T_s = 1/W$, where W is the channel bandwidth, and f_c is the center frequency. We assume a block fading channel in which the channel coefficients, *i.e.*, g_ks, remain constant during a block of length K symbols and change independently from a block to another one [12]. This is a good assumption for a UWB application, as its channel is under-spread. In [12] and [13] a frequency-domain model of the above UWB channel which is obtained by taking DFT from both sides of (2) is introduced. If $\boldsymbol{X} = (X_0, \ldots, X_{K-1})^T$ and $\boldsymbol{X'} = (X'_0, \ldots, X'_{K-1})^T$ denote the K-point DFT of the transmitted UWB signals from S to D and R to D, respectively and similarly, $\boldsymbol{Y} = (Y_0, \ldots, Y_{K-1})^T$ and $\boldsymbol{Y'} = (Y'_0, \ldots, Y'_{K-1})^T$ represent the DFT of the received signals at D and R, then using this frequency domain model we formulate the input–output relation $S \to R$ and $S \to D$ as

$$\begin{aligned} Y'_k &= \sqrt{K} G_k^{(2)} X_k + Z'_k, \\ Y_k &= \sqrt{K} G_k^{(1)} X_k + \sqrt{K} G_k^{(3)} X'_k + Z_k, \quad (k = 0, \ldots, K-1). \end{aligned} \qquad (4)$$

Here, $Z_k \sim \mathcal{CN}(0, N)$ and $Z'_k \sim \mathcal{CN}(0, N')$ are independent zero mean complex additive white Gaussian noise for the kth received sample. The vectors $\boldsymbol{G}^{(n)}$ $(n = 1, 2, 3)$ are the DFT of vectors of complex baseband channel coefficients $\boldsymbol{g}^{(n)} = (g_0^{(n)}, \ldots, g_{K-1}^{(n)})^T$ related to each link.

III. Upper and Lower Bounds on the Expected and Outage Capacities

In this section, we first derive the upper and lower bounds on the UWB channel capacity with a relay node for fixed channel coefficients. These results are the basis for the subsequent parts.

A. Upper Bound

The upper bound on a K-block delay constrained capacity of a relay channel has been derived in [3] as

$$C \le \max_{p(\boldsymbol{X}, \boldsymbol{X'})} \min \left\{ \frac{1}{K} \sum_{i=0}^{K-1} I(X_i, X'_i; Y_i), \frac{1}{K} \sum_{i=0}^{K-1} I(X_i; Y_i, Y'_i | X'_i) \right\} \qquad (5)$$

This bound is the tightest upper bound known to the authors. If we proceed similarly to [5], we can express this bound in terms of the power constraints and the UWB channel coefficients. In Appendix A, we have derived an upper bound for each of the mutual information terms in (5). Using these bounds ((A.2) and (A.6)), an upper bound on the capacity of our network when the UWB channel coefficients are known is obtained. This upper bound is given by (6) shown at the bottom of the page. In this equation, $\rho_i \triangleq \mathbb{E}\{X_i X_i'^*\}/E_s$ and the parameter E_s is the signal energy per complex baseband sample. We have also assumed that the source and relay nodes transmit their signals with equal energies, namely $|X_k| = |X'_k| = \sqrt{E_s}$.

B. Lower Bound

A lower bound on the capacity is given by [3]

$$C \ge \max_{p(\boldsymbol{X}, \boldsymbol{X'})} \min \left\{ \frac{1}{K} \sum_{i=0}^{K-1} I(X_i, X'_i; Y_i), \frac{1}{K} \sum_{i=0}^{K-1} I(X_i; Y'_i | X'_i) \right\} \qquad (7)$$

$$C \le \max_{\rho_0, \ldots, \rho_{K-1}} \min \left\{ \frac{1}{2K} \sum_{i=0}^{K-1} \log \left(1 + \frac{K E_s}{N} \left(\left| G_i^{(1)} \right|^2 + \left| G_i^{(3)} \right|^2 + 2\Re \left\{ G_i^{(1)} G_i^{(3)^*} \rho_i \right\} \right) \right), \right.$$
$$\left. \frac{1}{2K} \sum_{i=0}^{K-1} \log \left(1 + K \left(\frac{E_s}{N} \left| G_i^{(1)} \right|^2 + \frac{E_s}{N'} \left| G_i^{(2)} \right|^2 \right) \left(1 - |\rho_i|^2 \right) \right) \right\}. \qquad (6)$$

$$C \geq \frac{1}{2K} \max_{\rho_0,\ldots,\rho_{K-1}} \min \left\{ \sum_{i=0}^{K-1} \log\left(1+\frac{KE_s}{N'}\left|G_i^{(2)}\right|^2\left(1-|\rho_i|^2\right)\right), \right. \\ \left. \sum_{i=0}^{K-1} \log\left(1+\frac{KE_s}{N}\left(\left|G_i^{(1)}\right|^2+\left|G_i^{(3)}\right|^2+2\Re\left\{G_i^{(1)}G_i^{(3)^*}\rho_i\right\}\right)\right)\right\}. \quad (8)$$

$$C \leq \max_{\rho_0,\ldots,\rho_{K-1}} \min \left\{ \frac{1}{2}\log\left(1+\frac{E_s}{N}\sum_{i=0}^{K-1}\left|G_i^{(1)}\right|^2+\left|G_i^{(3)}\right|^2+2\Re\left\{G_i^{(1)}G_i^{(3)^*}\rho_i\right\}\right), \right. \\ \left. \frac{1}{2}\log\left(1+\sum_{i=0}^{K-1}\left(\frac{E_s}{N}\left|G_i^{(1)}\right|^2+\frac{E_s}{N'}\left|G_i^{(2)}\right|^2\right)\left(1-|\rho_i|^2\right)\right)\right\}. \quad (10)$$

The maximization is over the selection of joint probability mass function. So similar to the previous part, at first we have derived an upper bound on $I(X_i;Y_i'|X_i')$ in Appendix A ((A.8)). Now, from (A.2) and (A.8) in Appendix A and considering that these upper bounds are achieved by choosing (X_i, X_i') to be jointly Gaussian with correlation coefficient ρ_i, we simultaneously maximizes both mutual information terms. So the lower bound given in (8) is easily obtained.

C. Expected Capacity and Outage Capacity

The expected capacity is defined as $C_{\text{expected}} = \mathbb{E}\{C\}$where the expectation is taken over all channel realizations. Using the upper and lower bounds on C obtained in (6) and (8), respectively, the bounds on the expected capacity are obtained. The $p\%$ outage capacity is defined as [14]

$$C_{\text{outage}}(p) = \max\{C_0\} \quad \text{subject to} \quad \mathbb{P}\{C \geq C_0\} \geq 1-p. \quad (9)$$

where C is the delay constrained capacity conditioned on a specific channel parameter realization. The bounds on the outage capacity are obtained similarly as obtained for the expected capacity.

IV. Outage Probability Analysis

In this section we use the law of large numbers to express and approximate the upper bound on the capacity of the UWB channel with a relay node, derived in the previous section, in a very simplified form. Then, using this bound we obtain the outage probability.

A. Approximation for the Upper Bound (6)

By using Jensen's inequality, the upper bound (6) can be written as (10). As K is a very large number, we can approximate the term $\Re\left\{\sum_{i=0}^{K-1} G_i^{(1)}G_i^{(3)^*}\rho_i\right\}$ with $\Re\left\{K\,\mathbb{E}\left\{G_i^{(1)}G_i^{(3)^*}\rho_i\right\}\right\}$. For the time-domain channel coefficient defined in (3), we have $\mathbb{E}\{g_k\}=0$. As $\boldsymbol{G}^{(n)}$ is the DFT of $\boldsymbol{g}^{(n)}$, we conclude that $\mathbb{E}\left\{G_i^{(n)}\right\}$ is zero, too. Also $G_i^{(1)}$ and $G_i^{(3)}$ are independent, so $\mathbb{E}\left\{G_i^{(1)}G_i^{(3)^*}\rho_i\right\}=0$ and the effect of ρ_i's in the first term of the upper bound in (10) vanishes. Therefore (10) is maximized when $\rho_i = 0\,(i = 0,...,K-1)$. Considering this fact and also Parseval's relation $\sum_{i=0}^{K-1}\left|G_i^{(j)}\right|^2 = \sum_{i=0}^{K-1}\left|g_i^{(j)}\right|^2 = \sum_{i=0}^{K_j'-1}\left|g_i^{(j)}\right|^2$ $j=1,2,3$, where K_j' is the ISI length for jth link, we obtain

$$C \leq \min\left\{\frac{1}{2}\log\left(1+\frac{E_s}{N}\left(\sum_{i=0}^{K_1'-1}\left|g_i^{(1)}\right|^2+\sum_{i=0}^{K_3'-1}\left|g_i^{(3)}\right|^2\right)\right), \right. \\ \left. \frac{1}{2}\log\left(1+\sum_{i=0}^{K_1'-1}\frac{E_s}{N}\left|g_i^{(1)}\right|^2+\sum_{i=0}^{K_2'-1}\frac{E_s}{N'}\left|g_i^{(2)}\right|^2\right)\right\}. \quad (11)$$

From the SV (Saleh-Valenzuela) model for the UWB channel described in (1), if a pulse with duration T is transmitted, we receive the signal until $T_{L-1}+\tau_{M-1,L-1}+T$, where $T_{L-1}+\tau_{M-1,L-1}$ is the delay of the last ray in the last cluster. Therefore $K' = \frac{T_{L-1}+\tau_{M-1,L-1}+T}{T}$, which is a random variable with mean $\frac{\frac{L-1}{\Lambda}+(M-1)\left(\frac{\beta}{\lambda_1}+\frac{1-\beta}{\lambda_2}\right)}{T}+1$, where Λ is the cluster arrival rate, λ_1 and λ_2 are the ray arrival rates, and β is the mixing factor as defined in (1). Since $g_i^{(j)}$ is the sum of the taps of link j which appear in the interval $[iT,(i+1)T)$ and since T is typically less than the arrival time between the clusters and the rays in each cluster, with a good approximation we can assume $\sum_{i=0}^{K_j'-1}\left|g_i^{(j)}\right|^2 \simeq \frac{1}{\text{PL}_j}\sum_{m,\ell} {a_{m,\ell}^{(j)}}^2$ where PL_j is the pathloss of the jth link. In fact it is assumed that $\widetilde{\beta}$ (defined in (1)) models only the pathloss effect and the effect of shadowing and antenna insertion loss in $\widetilde{\beta}$ is ignored. Therefore

$$C \leq \min\left\{\frac{1}{2}\log\left(1+\text{SNR}\left(\sum_{m,\ell}{a_{m,\ell}^{(1)}}^2+\frac{\text{PL}_1}{\text{PL}_3}\sum_{m,\ell}{a_{m,\ell}^{(3)}}^2\right)\right), \right. \\ \left. \frac{1}{2}\log\left(1+\text{SNR}\left(\sum_{m,\ell}{a_{m,\ell}^{(1)}}^2+\frac{N}{N'}\frac{\text{PL}_1}{\text{PL}_2}\sum_{m,\ell}{a_{m,\ell}^{(2)}}^2\right)\right)\right\}. \quad (12)$$

where $\text{SNR} \triangleq \frac{1}{\text{PL}_1}\frac{E_s}{N}$ is the received signal to noise ratio of the direct link between the source and the destination. In Appendix B, we have computed $\mathbb{E}\left\{\sum_{m,\ell}a_{m,\ell}^2\right\}$. Using the results of this Appendix and applying Jensen's inequality again, the upper bound on the expected capacity of the relay network with UWB links is fully expressed versus UWB

channel parameters as

$$C_{\text{expected}} \leq \min\left\{\frac{1}{2}\log\left(1+\text{SNR}\left(A_1+\frac{\text{PL}_1}{\text{PL}_3}A_3\right)\right), \frac{1}{2}\log\left(1+\text{SNR}\left(A_1+\frac{N}{N'}\frac{\text{PL}_1}{\text{PL}_2}A_2\right)\right)\right\}, \quad (13)$$

where

$$A_i = \xi_i \exp\left(\frac{(\ln(10))^2}{200}\sigma^2_{cluster,i}\right)\kappa_i^{LOS} \cdot\frac{\phi_i'^{M_i}-1}{\phi_i'-1}\frac{\mu_i' e^{\bar{L}_i(\mu_i'-1)}-1}{\mu_i'-1} \qquad \text{for} \quad i=1,2,3 \quad (14)$$

The variable $\bar{L}_i$ denotes the mean number of clusters, M_i is the number of rays in each cluster, and $\sigma_{cluster,i}$ is the cluster shadowing variance of link i $(i=1,2,3)$. The parameters ξ_i and ϕ_i' are associated with the ray arrival rates and intra-cluster decay time constant and μ_i' is related to the inter-cluster arrival rate and decay time constant of link i. The coefficient κ_i^{LOS} depends on whether or not a line-of-sight (LOS) connection between the transmitter and receiver of link i exists. These terms are completely specified in the Appendix B.

B. Outage Probability

1) Special case 1 (Direct Link): As a first step in the calculation of outage probability of the UWB communication with a relay node, we consider a channel with mutual information

$$I = \frac{1}{2}\log\left(1+\text{SNR}\left(\sum_{k,\ell}a_{k,\ell}^2\right)\right). \quad (15)$$

This can be interpreted as a mutual information of a simple UWB link with channel coefficients $a_{k,\ell}$ (corresponding to the kth ray in ℓth cluster) which have Nakagami distribution with parameters $m_{k,\ell}$ and $\Omega_{k,\ell}$ fully defined in [6] and also in Appendix B. In our outage analysis, we compute the probability of outage conditioned on the arrival time of the received paths and Nakagami-m factor. Then, to derive the unconditional probability we take the expected value of the conditional probability. The sum of independent Nakagami coefficients in power terms in (15) can be approximated by an equivalent gamma distribution with the following parameters [15]

$$\Omega_e \simeq \sum_\ell\sum_k \Omega_{k,\ell}, \qquad m_e \simeq \frac{\left(\sum_\ell\sum_k\Omega_{k,\ell}\right)^2}{\sum_\ell\sum_k\frac{\Omega_{k,\ell}^2}{m_{k,\ell}}}. \quad (16)$$

Therefore the outage probability is computed as

$$P_{out} = \mathbb{P}\{I<R\} = \mathbb{P}\left\{z<\underbrace{\frac{2^{2R}-1}{\text{SNR}}}_{z_{th}}\right\} = \frac{\gamma\left(m_e, \frac{m_e z_{th}}{\Omega_e}\right)}{\Gamma(m_e)}, \quad (17)$$

where $z \triangleq \sum_{k,\ell}a_{k,\ell}^2$, $\Gamma(\cdot)$ is the gamma function, and $\gamma(\cdot,\cdot)$ is the lower incomplete gamma function.

The diversity order is a performance measurement which indicates how the slope of the probability of outage as a function of SNR changes. To compute the diversity order, we consider high SNR regime and use the identity $\gamma(a,b) = \int_0^b t^{a-1}e^{-t}dt = a^{-1}b^a e^{-b}M(1,a+1,b)$, where $M(.,.,.)$ is the confluent hypergeometric function with the following expression [16]

$$M(1,a+1,b) = 1+\frac{1}{(a+1)}b+\frac{1}{(a+1)(a+2)}b^2+\ldots \quad (18)$$

So with a good approximation P_{out} can be rewritten as

$$P_{out} = k_0\left(\frac{1}{\text{SNR}}\right)^{m_e}+k_1\left(\frac{1}{\text{SNR}}\right)^{m_e+1}+k_2\left(\frac{1}{\text{SNR}}\right)^{m_e+2}+\ldots \quad (19)$$

with $0<k_0\leq k_1\leq k_2\leq \ldots$. Now, it is obvious that at high SNR the first term on the right hand side of (19) is dominant. Thus, we obtain m_e-fold diversity gain, where m_e is defined in (16). If all the received paths have had the same Nakagami distribution parameters, namely $\Omega_{k,\ell}=\Omega_0$ and $m_{k,\ell}=m_0$, then we would have the diversity gain of m_0LM.

2) Special case 2: For the next step, consider a channel with mutual information

$$I = \frac{1}{2}\log\left(1+\text{SNR}\Big(\underbrace{\sum_{\ell=0}^{L_1-1}\sum_{k=0}^{M_1-1}a_{k,\ell}^2}_{z_1}+\alpha\underbrace{\sum_{\ell=0}^{L_2-1}\sum_{k=0}^{M_2-1}a_{k,\ell}'^2}_{z_2}\Big)\right), \quad (20)$$

where $a_{k,\ell}$ and $a'_{k,\ell}$ are Nakagami distributed random variables which are independent and α is a constant. Then z_1 and z_2, defined in (20), have a gamma distribution with parameters (m_1,Ω_1) and (m_2,Ω_2), which are obtained using (16). The probability of outage for this channel is

$$P_{out} = \mathbb{P}\{z_1+\alpha z_2<z_{th}\} = \mathcal{L}^{-1}\left(\frac{\Phi_{z_1+\alpha z_2}(-s)}{s}\right)\Bigg|_{z_{th}} = \mathcal{L}^{-1}\left(\frac{\Phi_{z_1}(-s)\Phi_{z_2}(-\alpha s)}{s}\right)\Bigg|_{z_{th}} \quad (21)$$

where z_{th} has been defined in (17), $\mathcal{L}^{-1}$ is the inverse Laplace transform, and $\Phi_{z_i}(s) = \left(1-s\frac{\Omega_i}{m_i}\right)^{-m_i}$ for $i=1,2$ [17]. We can also use the approximation given in (16) to approximate $z_1+\alpha z_2$ with a gamma distributed variable z' with parameters $m' \simeq \left((\Omega_1+\alpha\Omega_2)^2\right)\Big/\left(\frac{\Omega_1^2}{m_1}+\alpha^2\frac{\Omega_2^2}{m_2}\right)$ and $\Omega' \simeq \Omega_1+\alpha\Omega_2$. Then, the probability of outage is easily approximated as

$$P_{out} = \frac{\gamma\left(m', \frac{m' z_{th}}{\Omega'}\right)}{\Gamma(m')} \quad (22)$$

which gives us a diversity gain of m'. In a situation that all of the paths are Nakagami variables with similar parameters Ω_0 and m_0, and $\alpha=1$, then $\Omega_1=L_1M_1\Omega_0$ and $m_1=m_0L_1M_1$. Similarly $\Omega_2=L_2M_2\Omega_0$ and $m_2=m_0L_2M_2$ and therefore $m'=m_0\left(L_1M_1+L_2M_2\right)$.

3) UWB Channel with a Relay Node: An upper bound on the capacity of the UWB communication with a relay node has been derived previously in (12). This bound is the minimum of two mutual information terms

$$I_1 = \frac{1}{2}\log\left(1+\text{SNR}\left(\sum_{k,\ell}{a_{k,\ell}^{(1)}}^2+\frac{\text{PL}_1}{\text{PL}_3}\sum_{k,\ell}{a_{k,\ell}^{(3)}}^2\right)\right) \triangleq \frac{1}{2}\log\left(1+\text{SNR}\left(u_1+\alpha_3 u_3\right)\right)$$

$$I_2 = \frac{1}{2}\log\left(1+\mathrm{SNR}\left(\sum_{k,\ell} {a_{k,\ell}^{(1)}}^2 + \frac{N}{N'}\frac{\mathrm{PL}_1}{\mathrm{PL}_2}\sum_{k,\ell} {a_{k,\ell}^{(2)}}^2\right)\right) \triangleq \frac{1}{2}\log\left(1+\mathrm{SNR}\left(u_1+\alpha_2 u_2\right)\right), \quad (23)$$

each with their own outage probability P_{out1} and P_{out2}. In (23), u_i $(i = 1,2,3)$ is a gamma distributed variable with parameters Ω_i and m_i which are computed using (16), $\alpha_2 \triangleq \frac{N}{N'}\frac{\mathrm{PL}_1}{\mathrm{PL}_2}$ and $\alpha_3 \triangleq \frac{\mathrm{PL}_1}{\mathrm{PL}_3}$. Based on P_{out1} and P_{out2}, the overall system performance is evaluated [18]

$$\begin{aligned} P_{out} &\geq \mathbb{P}\{\min(I_1, I_2) < R\} \\ &\geq \max\left(\mathbb{P}\{I_1 < R\}, \mathbb{P}\{I_2 < R\}\right) \\ &= \max(P_{out1}, P_{out2}) \end{aligned} \quad (24)$$

where P_{out1} and P_{out2} are computed using (22). The amount of diversity gain is at most $\min(m_1, m_2)$. An improved lower bound is given by (25) which is obtained by eliminating the second inequality in (24). In this equation, $\Gamma(.,.)$ is the upper incomplete gamma function [16].

C. Performance Comparison

In this section, we explore some comparisons by considering the upper bound on the capacity of UWB channel with a relay node (12) and those of the UWB channel without a relay node and a narrowband channel with a relay node.
An upper bound on the capacity of a relay network with narrowband links is easily obtained as

$$C_{NB} \leq \min\left\{\frac{1}{2}\log\left(1+\mathrm{SNR}\left(|h_{sd}|^2 + \frac{\mathrm{PL}_1}{\mathrm{PL}_3}|h_{rd}|^2\right)\right), \frac{1}{2}\log\left(1+\mathrm{SNR}\left(|h_{sd}|^2 + \frac{N}{N'}\frac{\mathrm{PL}_1}{\mathrm{PL}_2}|h_{sr}|^2\right)\right)\right\}. \quad (26)$$

where h_{sd}, h_{rd} and h_{sr} are the channel coefficients between S-D, R-D and S-R, respectively.

From (12) and (26), an improvement when using UWB links comes from the diversity gain $\left(\sum_{m,\ell} {a_{m,\ell}}^2\right)$. In the UWB channel, extremely large bandwidth (> 1 GHz) enables the receiver to resolve a large number of paths. This multiple reception gives a diversity gain as we have observed in the previous section and leads to a more reliable system. We observed in section IV-B3 that the maximum diversity gain of the UWB communication with a relay node is equal to the minimum of two diversity gains which related to the combination of the relay links with the direct link between the source and the destination (24). This value is equal to $m_0L_1M_1 + \min(m_0L_2M_2, m_0L_3M_3)$ in the case of same Nakagami distribution parameters for three links and ignoring the pathloss effect. Considering high pathloss, this value is reduced to $\min(m_0L_2M_2, m_0L_3M_3)$ ((24) and (22) with large α) which is still substantially more than the diversity gain of at most 2 for the relay network with NB links [13].

The first differences between the UWB communication with and without a relay node is also in their diversity gains. In fact the UWB channel without a relay node corresponds to the channel which its mutual information was given in(15) and its diversity gain expressed in(19), while adding a relay node leads to a system with higher diversity gain((24)). To get some insight on the amount of increase in the diversity gain, consider a relay network with the links with similar Nakagami distribution parameters and ignore the pathloss. As stated before, the diversity gain of $m_0L_1M_1 + \min(m_0L_2M_2, m_0L_3M_3)$ is obtained for the UWB channel with a relay node; while this value degrades to $m_0L_1M_1$ when the relay node does not exist. It must be noticed that at high pathloss, where the former reduces to $\min(m_0L_2M_2, m_0L_3M_3)$, the diversity gain of the two cases is comparable. However, there still exists another advantage over the communications without a relay node. To this end, we apply Jensen's inequality to (12) and assume that the power of all paths of these three links are the same. So, it can be realized that adding a relay node to the UWB channel provides a power gain of $\min\left\{1+\frac{\mathrm{PL}_1}{\mathrm{PL}_3}, 1+\frac{N}{N'}\frac{\mathrm{PL}_1}{\mathrm{PL}_2}\right\}$. This power gain allows the source and the relay nodes to reduce their transmit powers for the same received SNR level [13] and it is very significant in the low SNR regime where UWB is supposed to work.

V. Capacity with a Constraint on the Transmitted Powers

In the previous sections, we assumed that the source and relay nodes transmit their signals with the same energy, namely $|X_k| = |X'_k| = \sqrt{E_s}$. In order to have a fair comparison with the UWB channel without a relay nodes, in this section we assume that the sum of the source and relay signal energies per complex baseband sample is equal to E_s. This total energy needs to be split in such a way that maximizes the achievable rate of the system. Let the parameter α denote the fraction of the energy allocated to the source, and hence $1-\alpha$ is the fraction of the energy allocated to the relay, namely $|X_i|^2 = \alpha E_s$ and $|X'_i|^2 = (1-\alpha)E_s$. To compute the aforementioned capacities, while we have this constraint, we proceed exactly as we have done in Appendix A and compute upper bounds on $I(X_i, X'_i; Y_i)$, $I(X_i; Y_i, Y'_i|X'_i)$, and $I(X_i; Y'_i|X'_i)$ considering this constraint. So the upper and lower bounds on the K-block delay constrained capacity of the UWB-relay network with fixed channel coefficients which are given by (27) and (28) are obtained. Using these equations, we can derive the bounds on the expected and outage capacities as it has been done in sections III-C. We can also apply similar approximation as what we used in IV-A to obtain simple upper bound. In the situation that the total powers of the paths in three links are the same, this approximation leads to the

$$\begin{aligned} P_{out} &\geq \mathbb{P}\{\min(I_1, I_2) < R\} = \mathbb{P}\{(I_1 < R) \cup (I_2 < R)\} = 1 - \mathbb{P}\{(I_1 \geq R) \cap (I_2 \geq R)\} \\ &= \frac{\gamma\left(m_1, \frac{m_1 z_{th}}{\Omega_1}\right)}{\Gamma(m_1)} - \int_0^{z_{th}} f_{u_1}(u_1)\frac{\Gamma\left(m_2, \frac{m_2}{\Omega_2}\frac{z_{th}-u_1}{\alpha_2}\right)}{\Gamma(m_2)}\frac{\Gamma\left(m_3, \frac{m_3}{\Omega_3}\frac{z_{th}-u_1}{\alpha_3}\right)}{\Gamma(m_3)}du_1 \end{aligned} \quad (25)$$

$$C \leq \max_{\alpha,\rho_0,\ldots,\rho_{K-1}} \min\left\{ \frac{1}{2K}\sum_{i=0}^{K-1} \log\left(1+\frac{KE_s}{N}\left(\alpha\left|G_i^{(1)}\right|^2+(1-\alpha)\left|G_i^{(3)}\right|^2+2\sqrt{\alpha(1-\alpha)}\Re\left\{G_i^{(1)}G_i^{(3)^*}\rho_i\right\}\right)\right), \right.$$
$$\left. \frac{1}{2K}\sum_{i=0}^{K-1} \log\left(1+\frac{\alpha KE_s}{NN'}\left(N'\left|G_i^{(1)}\right|^2+N\left|G_i^{(2)}\right|^2\right)\left(1-|\rho_i|^2\right)\right)\right\}. \quad (27)$$

$$C \geq \max_{\alpha,\rho_0,\ldots,\rho_{K-1}} \min\left\{ \frac{1}{2K}\sum_{i=0}^{K-1} \log\left(1+\frac{KE_s}{N}\left(\alpha\left|G_i^{(1)}\right|^2+(1-\alpha)\left|G_i^{(3)}\right|^2+2\sqrt{\alpha(1-\alpha)}\Re\left\{G_i^{(1)}G_i^{(3)^*}\rho_i\right\}\right)\right), \right.$$
$$\left. \frac{1}{2K}\sum_{i=0}^{K-1} \log\left(1+\frac{\alpha KE_s}{N'}\left|G_i^{(2)}\right|^2\left(1-|\rho_i|^2\right)\right)\right\}. \quad (28)$$

optimal power allocation of $\alpha_{Opt.} \simeq \frac{\mathrm{PL}_2}{\mathrm{PL}_2+\frac{N}{N'}\mathrm{PL}_3}$. That is by moving the relay node toward the destination, more power is allocated to the source, namely $\alpha \to 1$. On the other hand, when the relay node moves to the source $\alpha \to 0$, the relay node transmits with more power compared with the source.

VI. Numerical Results

In this section, we present some numerical results for the derived bounds on the expected and 10% outage capacities and the system outage probability. We consider a NLOS scenario in a residential environment with $3\,\mathrm{GHz}$ bandwidth and center frequency of $6\,\mathrm{GHz}$. The values of the channel parameters have been taken from [6]. In our plots, we have considered the pathloss as a function of distance and ignored its frequency dependency

$$\mathrm{PL}(d) = \mathrm{PL}_0 + 10n\log_{10}\left(\frac{d}{d_0}\right), \quad (29)$$

where the reference distance d_0 is set to $1\,\mathrm{m}$, PL_0 is the pathloss at the reference distance and n is the pathloss exponent, which also depends on the environment and whether or not LOS exists. The distance d_1 between the source and the destination has been set to $3\,\mathrm{m}$, and we assume that the relay is moved along a direct line between them. Furthermore, it is assumed that the transmitted powers by the source and the relay nodes are at most equal to the maximum allowed power for the UWB systems which is stipulated by FCC ($-41.3\,\mathrm{dBm/MHz}$). Assuming the noise power spectral density of $-114\,\mathrm{dBm/MHz}$, the received SNR at distance $3\,\mathrm{m}$ for the above scenario becomes $2.1\,\mathrm{dB}$. Finally in the plots we have assumed equal average fading power of 1 for three links (averaged over all the different random processes).

Fig. 1 depicts the lower bounds (LB) on the expected and 10% outage capacities of our network and compares these capacities with the capacity of a UWB channel without a relay node. In this figure, the relay node is exactly in the middle between the source and the destination. As can be realized, significant increase in the expected and outage capacities is obtained using a relay node. For example at $\mathrm{SNR} = -4\,\mathrm{dB}$ we have more than five fold increase in the expected capacity[2]. This superiority is more for the outage capacity. It must be noticed that when SNR decreases, as expected both the outage and expected capacities decrease; but the amount of improvement in both capacities substantially increases by using a relay node. In the other words, the improvement is more considerable in the low SNR regime, where the UWB is supposed to operate.

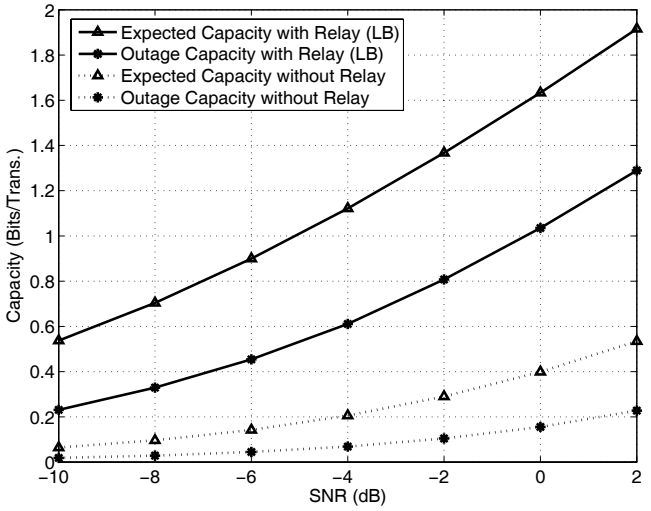

Fig. 1. Lower bounds on the expected and 10% outage capacities of a UWB-linked relay network vs. SNR.

In Fig. 2, the effect of the relay's position and the individual quality of each link on the capacity are demonstrated. This figure presents the expected capacity for different noise level differences $\Delta = N - N'$ at a bandwidth of $3\,\mathrm{GHz}$ and SNR of $2.1\,\mathrm{dB}$, where N and N' are defined in (4). As this figure shows, there is an optimum point for the position of the relay between the source and the destination, in which the capacity is maximized. It can be seen that the shape of the resulting bound on the capacity is not symmetric. According to (5), the capacity is the minimum of the two expressions for mutual information $I(X_i, X_i'; Y_i)$ and $I(X_i; Y_i, Y_i'|X_i')$.

[2]Note that to provide numerical bounds on the capacities in units of "bit/channel use", we must divide the results for the system with a relay node by 2. This is due to the fact that when utilizing a relay node, we are in fact using the channel twice, while without a relay the channel is used just once.

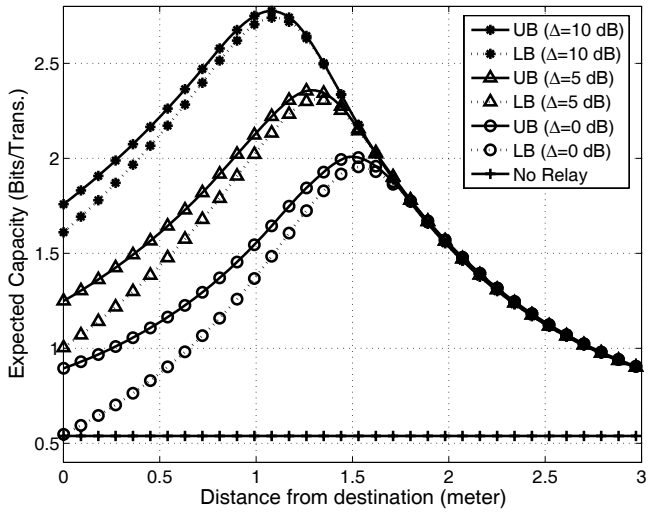

Fig. 2. Upper and lower bounds on the expected capacity of a UWB-linked relay network vs. relay's distance from the destination.

The left branch of the expected capacity curves are attributed to $I(X_i; Y_i, Y_i'|X_i')$, whereas the right part is mostly due to $I(X_i, X_i'; Y_i)$. In the case of an equal signal to noise ratio on all links, *i.e.*, $\Delta = 0\,\mathrm{dB}$, this optimum point for the expected capacity is at $d = 1.5\,\mathrm{m}$. Also it can be observed that by the decrement of the relay's noise, the capacity increases and the relay's optimum position moves towards the destination. Fig. 2 also shows that the derived upper and lower bounds are tight specially when the relay is not too near to the destination.

We investigate the effect of applying the constraint on the total source and relay powers on the expected capacity in Fig. 3. The lower bound on the expected capacity and the optimum fraction of the power allocated to the source for different value of Δ are plotted in Figs. 3(a), 3(b) respectively. We have also presented the lower bound on the expected capacity for constant $\alpha = 0.5$ and $\Delta = 0\,\mathrm{dB}$. This comparison is fairer compared to the results of Fig. 2, since the total power transmitted toward the destination is the same for both with and without relay nodes. Here, the capacity increases by a factor of 2.9 when the relay node is in the middle of the source and destination (for similar situation, but without power constraint, it was 3.7 (Fig. 2)).

Next, we consider a scenario in which the distance between the source and the destination (d_1) varies from $1\,\mathrm{m}$ to $5\,\mathrm{m}$ (Fig. 4). It is assumed that the source transmits its signals with the same power for different values of d_1 (with the maximum allowed power for UWB communication by FCC). Also relay node is exactly in the middle between the source and the destination. As we expect, at the constant SNR, the capacity of UWB channel (with and without a relay node) decreases when d_1 increases. We can also observe that the amount of improvement when using a relay node increases with d_1. For example at the distance $d_1 = 1\,\mathrm{m}$ the capacity improves by a factor of 1.6 when we have a relay node, while for the case of $d_1 = 5\,\mathrm{m}$ we have more than seven fold increase in the capacity using a relay node.

Fig. 5 shows the derived lower bounds on the outage probability of the UWB communication with and without a relay node. To examine the accuracy of the analytical expression derived for the outage probability and confirm the theoretical analysis, simulation results obtained by Monte Carlo method are also provided in this figure. In these plots we set $R = 1\,\mathrm{bps/Hz}$. The superior outage probability performance of the UWB communication with the aid of a relay node over that without a relay node is obvious in this figure. This improvement increases as SNR increases. Also it can be observed from Fig. 5 that the simulation results follow the analytical results obtained in section IV-B.3.

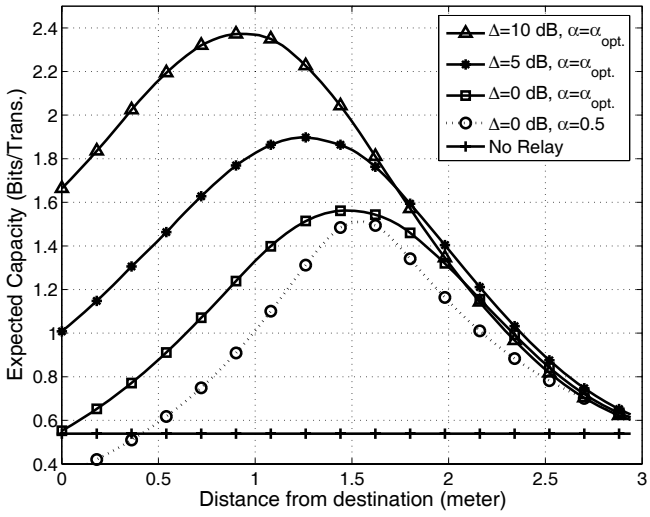

(a)

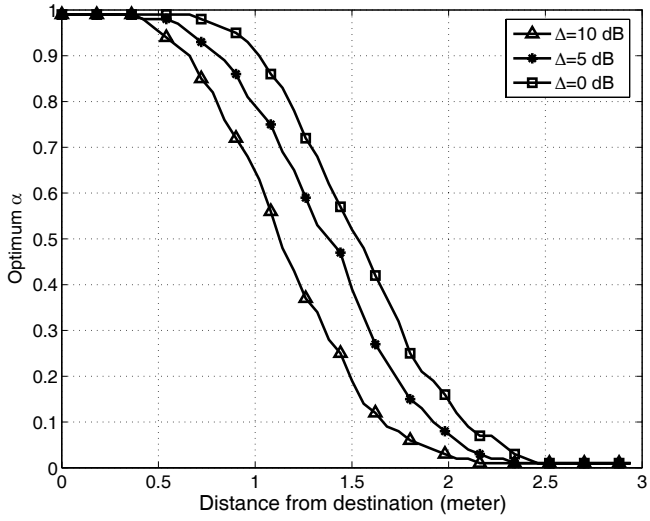

(b)

Fig. 3. Lower bounds on the expected capacity of a UWB-linked relay network vs. relay's distance from the destination with a constraint on the transmitted power. a) Expected capacity, b) Corresponding $\alpha_{Opt.}$.

VII. Conclusion

We computed bounds on the expected and outage capacities of a three-node relay network with UWB links versus channel coefficients and transmitted powers. We also developed a simple tight approximation for the derived upper bound on the capacity which was the basis for the outage probability analysis. It was shown that the diversity gain of a relay channel

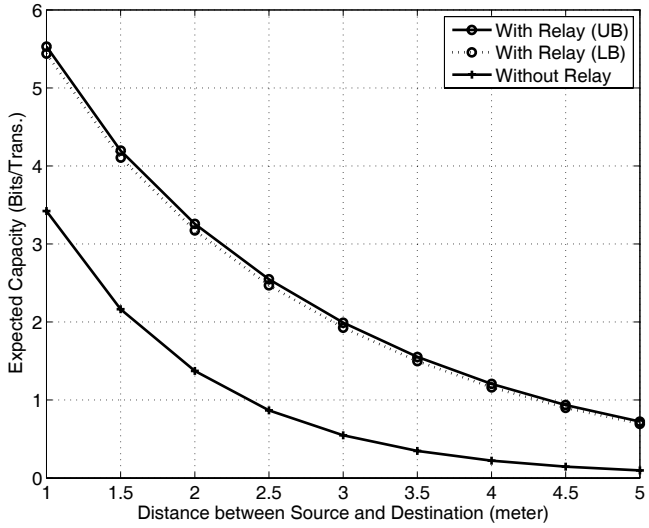

Fig. 4. Bounds on the expected capacity of a UWB-linked relay network vs. distance between source and destination (d_1).

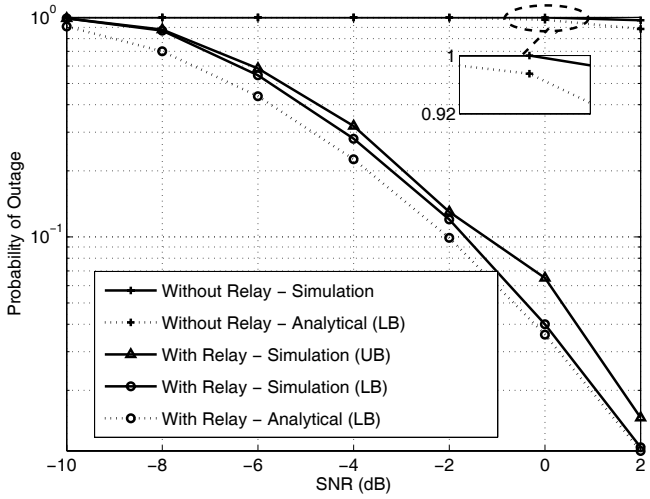

Fig. 5. Bounds on the probability of outage of a UWB-linked relay network vs. SNR.

increases significantly by using UWB links instead of NB links. Furthermore, the bounds on the capacity of the network were derived when there was a constraint on the transmitted powers of the source and relay node.

APPENDIX A

A. Upper Bound on $I(X_i, X_i'; Y_i)$

The mutual information $I(X_i, X_i'; Y_i)$ is expressed through the difference between entropies $h(Y_i)$ and $h(Y_i|X_i, X_i')$. An upper bound on the entropy $h(Y_i)$ is obtained similar to [5] as

$$h(Y_i) \le \mathbb{E}\left\{\frac{1}{2}\log(2\pi\mathrm{e}\ \mathrm{var}(Y_i))\right\} \le \frac{1}{2}\log\left(2\pi\mathrm{e}\left(KE_s\left(\left|G_i^{(1)}\right|^2+\left|G_i^{(3)}\right|^2\right)+2KE_s\Re\left\{G_i^{(1)}G_i^{(3)^*}\rho_i\right\}+N\right)\right) \quad \text{(A.1)}$$

where $\rho_i \triangleq \mathbb{E}\{X_i X_i'^*\}/E_s$ and the parameter E_s is the signal energy per complex baseband sample. The second term, *i.e.,* $h(Y_i|X_i, X_i')$ is equal to $\frac{1}{2}\log(2\pi\mathrm{e}N)$ [19]. So an upper bound on $I(X_i, X_i'; Y_i)$ is obtained by

$$I(X_i, X_i'; Y_i) \le \frac{1}{2}\log\left(1+\frac{KE_s}{N}\left(\left|G_i^{(1)}\right|^2+\left|G_i^{(3)}\right|^2+2\Re\left\{G_i^{(1)}G_i^{(3)^*}\rho_i\right\}\right)\right). \quad \text{(A.2)}$$

B. Upper Bound on $I(X_i; Y_i, Y_i'|X_i')$

We know that

$$I(X_i; Y_i, Y_i'|X_i') = h(Y_i|X_i') + h(Y_i'|Y_i, X_i') - h(Y_i, Y_i'|X_i, X_i'). \quad \text{(A.3)}$$

The upper bounds for the first two terms on the right hand side are as follows

$$h(Y_i|X_i') \le \frac{1}{2}\log\left(2\pi\mathrm{e}\left(\mathbb{E}\{|Y_i|^2\}-\frac{|\mathbb{E}\{Y_i X_i'^*\}|^2}{\mathbb{E}\{|X_i'|^2\}}\right)\right) = \frac{1}{2}\log\left(2\pi\mathrm{e}\left(KE_s\left|G_i^{(1)}\right|^2(1-|\rho_i|^2)+N\right)\right), \quad \text{(A.4)}$$

and

$$h(Y_i'|Y_i, X_i') \le \frac{1}{2}\log\left(2\pi\mathrm{e}\frac{KE_s\left(N'\left|G_i^{(1)}\right|^2+N\left|G_i^{(2)}\right|^2\right)(1-|\rho_i|^2)+NN'}{KE_s\left|G_i^{(1)}\right|^2(1-|\rho_i|^2)+N}\right) \quad \text{(A.5)}$$

We also know that $h(Y_i, Y_i'|X_i, X_i') = \frac{1}{2}\Big(\log(2\pi\mathrm{e}N) + \log(2\pi\mathrm{e}N')\Big)$. Therefore

$$I(X_i; Y_i, Y_i'|X_i') \le \frac{1}{2}\log\left(1+KE_s(1-|\rho_i|^2)\left(\frac{\left|G_i^{(1)}\right|^2}{N}+\frac{\left|G_i^{(2)}\right|^2}{N'}\right)\right). \quad \text{(A.6)}$$

C. Upper Bound on $I(X_i; Y_i'|X_i')$

As we know $I(X_i; Y_i'|X_i')$ is equal to the difference between $h(Y_i'|X_i')$ and $h(Y_i'|X_i, X_i')$. But

$$h(Y_i'|X_i') \le \frac{1}{2}\log\left(2\pi e\left(KE_s\left|G_i^{(2)}\right|^2\left(1-|\rho_i|^2\right)+N'\right)\right). \quad \text{(A.7)}$$

and $h(Y_i|X_i, X_i') = \frac{1}{2}\log(2\pi eN')$. Therefore

$$I(X_i; Y_i'|X_i') \le \frac{1}{2}\log\left(1+\frac{KE_s}{N'}\left|G_i^{(2)}\right|^2(1-|\rho_i|^2)\right). \quad \text{(A.8)}$$

APPENDIX B

In this appendix, we compute the expected value of $\sum_{m,\ell} a_{m,\ell}{}^2$ versus UWB channel parameters, where for

notational simplicity the index i which stands for the ith link has been suppressed. The channel coefficient $a_{m,\ell}$ has Nakagami distribution with parameters $m_{k,\ell}$ and $\Omega_{k,\ell} = \frac{1}{\gamma_\ell[(1-\beta)\lambda_1+\beta\lambda_2+1]} e^{\left(-\frac{\tau_{k,\ell}}{\gamma_\ell}\right)} e^{\left(-\frac{T_\ell}{\Gamma}\right)} 10^{\frac{M_{cluster}}{10}}$, in which T_ℓ is the arrival time of the ℓth cluster and $\tau_{k,\ell}$ is the arrival time of the kth ray in the ℓth cluster relative to the cluster arrival time T_ℓ. $M_{cluster}$ is a zero mean normally distributed variable with standard deviation $\sigma_{cluster}$, γ_ℓ and Γ are the decay rates and mean energy of each cluster and λ_1, λ_2 and β are defined in (11). So

$$\mathbb{E}\left\{\sum_{\ell=0}^{L-1}\sum_{m=0}^{M-1}|a_{m,\ell}|^2\right\} = \mathop{\mathbb{E}}_{L,T_\ell,\tau_{m,\ell},\ldots}\left\{\mathop{\mathbb{E}}_{a_{m,\ell}}\left\{\sum_{\ell=0}^{L-1}\sum_{m=0}^{M-1}|a_{m,\ell}|^2\right\}\right\}$$
$$= \mathop{\mathbb{E}}_{L,T_\ell,\tau_{m,\ell},\ldots}\left\{\sum_{\ell,m}\zeta_\ell e^{-\frac{\tau_{m,\ell}}{\gamma_\ell}} e^{-\frac{T_\ell}{\Gamma}}\right\}, \quad \text{(B.1)}$$

where $\zeta_\ell \triangleq \frac{1}{\gamma_\ell[(1-\beta)\lambda_1+\beta\lambda_2+1]} 10^{\frac{M_{cluster}}{10}}$. In the second step, we take the expectation with respect to $\tau_{m,\ell}$. To this end, we rewrite $\tau_{m,\ell}$ as $\tau_{m,\ell} = \sum_{j=1}^{m}\varepsilon_{j,\ell}$, where $\varepsilon_{j,\ell}$ is the interarrival time between rays j and $j-1$ in the ℓth cluster [20] (note that by definition $\tau_{0,\ell} = 0$). Then it can be easily observed that $\varepsilon_{j,\ell}$s are i.i.d random variables with probability density function of $p(\varepsilon_{j,\ell}) = \beta\lambda_1 e^{(-\lambda_1\varepsilon_{j,\ell})} + (1-\beta)\lambda_2 e^{(-\lambda_2\varepsilon_{j,\ell})}$. So

$$\mathbb{E}\left\{\sum_{\ell=0}^{L-1}\sum_{m=0}^{M-1}|a_{m,\ell}|^2\right\} = \mathop{\mathbb{E}}_{L,T_\ell,\ldots}\left\{\sum_{\ell,m}\zeta_\ell e^{\left(\frac{-T_\ell}{\Gamma}\right)}\prod_{j=1}^{m}\mathop{\mathbb{E}}_{\varepsilon_{j,\ell}}\left\{e^{-\frac{\varepsilon_{j,\ell}}{\gamma_\ell}}\right\}\right\}$$
$$= \mathop{\mathbb{E}}_{L,T_\ell,\ldots}\left\{\sum_{\ell}\zeta_\ell e^{(-T_\ell/\Gamma)}\frac{\phi_\ell'^M-1}{\phi_\ell'-1}\right\} \quad \text{(B.2)}$$

where $\phi_\ell' = \frac{\beta\lambda_1}{\lambda_1+1/\gamma_\ell} + \frac{(1-\beta)\lambda_2}{\lambda_2+1/\gamma_\ell}$. Even though, γ_ℓ is found to depend linearly on the arrival times of the clusters; but in the parametrization that is based on some measurements, its slope usually takes the value of zero [6]. So we can assume that $\gamma_\ell = \gamma_0$ and omit the dependency of ζ_ℓ and ϕ_ℓ' to ℓ. Now we take the expected value respect to T_ℓ. Similar to the previous step, let ϵ_j which is modeled as an exponential random variable with parameter Λ, denotes the time interval between clusters j and $j-1$. We have $T_\ell = \sum_{j=0}^{\ell}\epsilon_j$ (note that here $\epsilon_0 = 0$ if we have LOS scenario else it obeys the exponential distribution).

$$\mathbb{E}\left\{\sum_{\ell=0}^{L-1}\sum_{m=0}^{M-1}|a_{m,\ell}|^2\right\} = \mathop{\mathbb{E}}_{L,\epsilon_0,M_{cluster}}\left\{\zeta\frac{\phi'^M-1}{\phi'-1}\mathop{\mathbb{E}}_{T_\ell}\left\{\sum_{\ell}e^{(-T_\ell/\Gamma)}\right\}\right\}$$
$$= \mathop{\mathbb{E}}_{L,\ldots}\left\{\zeta\frac{\phi'^M-1}{\phi'-1}e^{\left(-\frac{\epsilon_0}{\Gamma}\right)}\frac{\mu'^L-1}{\mu'-1}\right\} \quad \text{(B.3)}$$

where $\mu' = \frac{\Lambda}{\Lambda+1/\Gamma}$. Now by taking the expected value respect to the rest parameters we obtain

$$\mathbb{E}\left\{\sum_{\ell=0}^{L-1}\sum_{m=0}^{M-1}|a_{m,\ell}|^2\right\} = \xi\exp\left(\frac{(\ln(10))^2}{200}\sigma_{cluster}^2\right)\kappa^{LOS}$$
$$\cdot\frac{\phi'^M-1}{\phi'-1}\frac{\mu' e^{\bar{L}(\mu'-1)}-1}{\mu'-1} \quad \text{(B.4)}$$

where $\xi \triangleq \frac{1}{\gamma_0[(1-\beta)\lambda_1+\beta\lambda_2+1]}$ and κ^{LOS} is equal to 1 for LOS connection and equal to μ' for NLOS connection. Now considering (B.4) and applying Jensen's inequality to (12), the upper bound on the K-block delay constrained expected capacity of a relay network with UWB links is completely expressed versus UWB channel parameters.

REFERENCES

[1] A. Sendonaris, E. Erkip, and B. Aazhang, "User cooperation diversity—part I: system description," *IEEE Trans. Commun.*, vol. 51, no. 11, pp. 1927–1938, Nov. 2003.

[2] A. Ribeiro and G. Giannakis, "Fixed and random access cooperative networks," *EURASIP News Letter*, vol. 17, no. 1, pp. 3–24, Mar. 2006.

[3] T. Cover and A. E. Gamal, "Capacity theorems for the relay channel," *IEEE Trans. Inform. Theory*, vol. IT-25, no. 5, pp. 572–584, Sept. 1979.

[4] A. E. Gamal and M. Aref, "The capacity of the semi-deterministic relay channel," *IEEE Trans. Inform. Theory*, vol. IT-28, no. 3, p. 536, May 1982.

[5] M. Khojastepour, A. Sabharwal, and B. Aazhang, "On capacity of Gaussian 'cheap' relay channel," in *Proc. IEEE Globecom Conference*, Dec. 2003, pp. 1776–1780.

[6] A. F. Molisch, C. C. Chong, B. Kannan, S. Emami, A. Fort, J. Karedal, and U. G. Schuster, "802.15.4a channel model subgroup final report, IEEE 802.15-04-0535-00-004a," Berlin, Germany, Sept. 2004.

[7] E. Biglieri, J. Proakis, and S. Shamai(Shitz), "Fading channel: information theoretic and communication aspects," *IEEE Trans. Inform. Theory*, vol. 44, pp. 2619–2692, Oct. 1998.

[8] A. S. Avestimehr and D. N. C. Tse,"Outage capacity of the fading relay channel in the low-snr regime," *IEEE Trans. Inf. Theory*, vol. 53, pp. 1401-1415, Apr. 2007.

[9] B. Wang, J. Zhang, and L. Zheng,"Achievable rates and scaling laws of power-constrained wireless sensory relay networks," *IEEE Trans. Inf. Theory*, vol. 52, pp. 4084-4104, 2006.

[10] T. Q. S. Quek, M. Z. Win, and M. Chiani, "Distributed diversity in ultrawide bandwidth wireless sensor networks," in *Proc. Vehicular Technology Conference*, June 2005, pp. 1355–1359.

[11] D. Cassioli, M. Z. Win, and A. F. Molisch, "The ultra-wide bandwidth indoor channel: from statistical model to simulations," *IEEE J. Sel. Areas Commun.*, vol. 20, pp. 1247-1257, Aug. 2002.

[12] E. Arikan, "Capacity bounds for an ultra-wideband channel model," in *Proc. IEEE ITW Conference*, Oct. 2004, pp. 176–181.

[13] D. Tse and P. Viswanath, *Fundamentals of Wireless Communication*. Cambridge University Press, 2004.

[14] A. Host-Madsen and J. Zhang, "Capacity bounds and power allocation for wireless relay channels," *IEEE Trans. Inf. Theory*, vol. 51, no. 6, pp. 2020-2040, June 2005.

[15] J. Reig and N. Cardona, "Approximation of outage probability on nakagami fading channels with multiple interference," *Electron. Lett.*, vol. 36, no. 19, pp. 1649–1650, Sept. 2000.

[16] M. Abramowitz and I. A. Stegun, *Handbook of Mathematical Functions With Formulas, Graphs, and Mathematical Tables*. New York: Dover, 1965.

[17] M. Dohler and H. Aghvami, "Information outage probability of distributed stbcs over nakagami fading channels," *IEEE Commun. Lett.*, vol. 8, no. 7, pp. 437–439, July 2004.

[18] E. Stauffer, O. Oyman, R. Narasimhan, and A. Paulraj, "Finite-SNR diversity-multiplexing tradeoffs in fading relay channels," *IEEE J. Select. Areas Commun.*, vol. 25, no. 2, pp. 245–257, Feb. 2007.

[19] T. Cover and J. Thomas, *Elements of Information Theory*. Wiley Inc., 1991.

[20] W. P. Siriwongpairat, W. Su, M. Olfat, and K. J. R. Liu, "Multiband-OFDM MIMO coding framework for UWB communication systems," *IEEE Trans. Signal Processing*, vol. 54, no. 1, pp. 214–224, Jan. 2006.